

FINITE ELEMENT ANALYSIS OF NON LINEAR DENSITY-TEMPERATURE VARIATION ON NON-DARCY CONVECTIVE HEAT TRANSFER FLOW IN A VERTICAL CHANNEL

C. Sulochana, Sharanamma V A*

Dept. of Mathematics, Gulbarga University, Gulbarga, India

(Received on: 27-09-12; Revised & Accepted on: 28-10-12)

ABSTRACT

We attempt to study the effect of quadratic density-temperature variation on non-Darcy convective Heat transfer flow of a viscous fluid through a porous medium in a vertical channel with heat generating sources. The governing equations flow, heat transfer are solved by using Galerkin finite element technique with quadratic polynomial approximations. The approximation solution is written directly as a linear combination of approximation functions with unknown nodal values as coefficients. Secondly, the approximation polynomials are chosen exclusively from the lower order piecewise polynomials restricted to contiguous elements. The velocity, temperature, , shear stress and rate of Heat transfer are evaluated numerically for different variations of parameter

Keywords: Magnetic field, Heat Transfer, Porous Medium, density –temperature and Finite Element Analysis.

1. INTRODUCTION

Non – Darcy effects on natural convection in porous media have received a great deal of attention in recent years because of the experiments conducted with several combinations of solids and fluids covering wide ranges of governing parameters which indicate that the experimental data for systems other than glass water at low Rayleigh numbers, do not agree with theoretical predictions based on the Darcy flow model. This divergence in the heat transfer results has been reviewed in detail in Cheng (13) among others. Extensive effects are thus being made to include the inertia and viscous diffusion terms in the flow equations and to examine their effects in order to develop a reasonable accurate mathematical model for convective transport in porous media. The work of Vafai and Tien (10) was one of the early attempts to account for the boundary and inertia effects in the momentum equation for a porous medium. They found that the momentum boundary

layer thickness is of order of $\sqrt{\frac{k}{\epsilon}}$. Vafai and Thiyagaraja (11) presented analytical solutions for the velocity and temperature fields for the interface region using the Brinkman Forchheimer –extended Darcy equation. Detailed accounts of the recent efforts on non-Darcy convection have been recently reported in Tien and Hong (3), cheng (14), and Kladias and Prasad (12). Here, we will restrict our discussion to the vertical cavity only. Poulikakos and Bejan (4, 5) investigated the inertia effects through the inclusion of Forchheimer’s velocity squared term, and presented the boundary layer analysis for tall cavities. They also obtained numerical results for a few cases in order to verify the accuracy of their boundary layer analysis for tall cavities. They also obtained numerical results for a few cases in order to verify the accuracy of their boundary layer solutions. This result in reversal of flow regimes from boundary layer to asymptotic to conduction as the contribution of the inertia term increases in comparison with that of the boundary term. They also reported a criterion for the Darcy flow limit.

The Brinkman – Extended – Darcy modal was considered in Tong and Subramanian (15), and Lauriat and Prasad (6) to examine the boundary effects on free convection in a vertical cavity. While Tong and Subramanian performed a Weber – type boundary layer analysis, Lauriat and Prasad solved the problem numerically for A=1 and 5. It was shown that for a fixed modified Rayleigh number, Ra, the Nusselt number; decrease with an increase in the Darcy number; the reduction being larger at higher values of Ra. A scale analysis as well as the computational data also showed that the transport term $(v \cdot \nabla) v$, is of low order of magnitude compared to the diffusion plus buoyancy terms (6). A numerical study based on the Forchheimer-Brinkman-Extended Darcy equation of motion has also been reported recently by Beckerman et al (2). They demonstrated that the inclusion of both the inertia and boundary effects is important for convection in a rectangular packed – sphere cavity.

Corresponding author: C. Sulochana, Sharanamma V A*
Dept. of Mathematics, Gulbarga University, Gulbarga, India

Keeping the above application in view we made attempt in this paper to study effect of quadratic density-temperature on non-Darcy convective heat transfer flow of a viscous fluid through a porous medium in a vertical channel with heat generating sources. The governing equations flow, heat transfer are solved by using Galerkin finite element technique with quadratic polynomial approximations. The approximation solution is written directly as a linear combination of approximation functions with unknown nodal values as coefficients. Secondly, the approximation polynomials are chosen exclusively from the lower order piecewise polynomials restricted to contiguous elements. The velocity, temperature, shear stress and rate of Heat transfer are evaluated numerically for different variations of parameter.

2. FORMULATION OF THE PROBLEM

We consider a fully developed laminar convective heat transfer flow of a viscous, electrically conducting fluid through a porous medium confined in a vertical channel bounded by flat walls. We choose a Cartesian co-ordinate system $O(x, y, z)$ with x -axis in the vertical direction and y -axis normal to the walls. The walls are taken at $y = \pm 1$. The walls are maintained at constant temperature. The temperature gradient in the flow field is sufficient to cause natural convection in the flow field. A constant axial pressure gradient is also imposed so that this resultant flow is a mixed convection flow. The porous medium is assumed to be isotropic and homogeneous with constant porosity and effective thermal diffusivity. The thermo physical properties of porous matrix are also assumed to be constant and Boussinesq approximation is invoked by confining the density variation to the buoyancy term. In the absence of any extraneous force flow is unidirectional along the x -axis which is assumed to be infinite.

The Brinkman-Forchheimer-extended Darcy equation which account for boundary inertia effects in the momentum equation is used to obtain the velocity field. Based on the above assumptions the governing equations are

$$-\frac{\partial p}{\partial x} + \left(\frac{\mu}{\delta}\right) \frac{\partial^2 u}{\partial y^2} - \left(\frac{\mu}{k}\right) u - \left(\frac{\sigma \mu_e^2 H_o^2}{\rho_o}\right) u + \frac{\rho \delta F}{\sqrt{k}} u^2 + \beta g(T - T_0) + \beta_1 g(T - T_0)^2 = 0 \quad (2.1)$$

$$\rho_0 C_p u \frac{\partial T}{\partial x} = \lambda \frac{\partial^2 T}{\partial y^2} + Q(T_0 - T) \quad (2.2)$$

The boundary conditions are

$$\begin{aligned} u = 0, \quad T = T_1 & \quad \text{on } y = -L \\ u = 0, \quad T = T_2 & \quad \text{on } y = +L \end{aligned} \quad (2.3)$$

The axial temperature gradient $\frac{\partial T}{\partial x}$ are assumed to be constant, say, A

where u is the velocity, T , is the temperature, p is the pressure, ρ is the density of the fluid, C_p is the specific heat at constant pressure, μ is the coefficient of viscosity, k is the permeability of the porous medium, δ is the porosity of the medium, β is the coefficient of thermal expansion, λ is the coefficient of thermal conductivity, F is a function that depends on the Reynolds number and the microstructure of porous medium, J is the current density vector, H is the magnetic field vector, and Q is the strength of the heat generating source. Here, the thermo physical properties of the solid and fluid have been assumed to be constant except for the density variation in the body force term (Boussinesq approximation) and the solid particles and the fluids are considered to be in the thermal equilibrium).

We define the following non-dimensional variables as

$$u' = \frac{u}{(v/L)}, \quad (x', y') = (x, y)/L, \quad p' = \frac{p\delta}{(\rho v^2/L^2)}, \quad \theta = \frac{T - T_2}{T_1 - T_2} \quad (2.4)$$

Introducing these non-dimensional variables the governing equations in the dimensionless form reduce to (on dropping the dashes)

$$\frac{d^2 u}{dy^2} = \pi + \delta(D^{-1} + M^2)u + \delta^2 \Delta u^2 - \delta G(\theta + \gamma \theta^2) \quad (2.5)$$

$$\frac{d^2 \theta}{dy^2} - \alpha \theta = (PN_T)u \quad (2.6)$$

where

$$\Delta = FD^{-1/2} \quad (\text{Inertia or Fochhemeir parameter})$$

$$G = \frac{\beta g (T_1 - T_2) L^3}{\nu^2} \quad (\text{Grashof Number})$$

$$D^{-1} = \frac{L^2}{k} \quad (\text{Darcy parameter})$$

$$P = \frac{\mu C_p}{\lambda} \quad (\text{Prandtl Number})$$

$$\alpha = \frac{QL^2}{\lambda} \quad (\text{Heat source parameter})$$

$$N_T = \frac{AL}{(T_1 - T_2)} \quad (\text{Temperature gradient})$$

The corresponding boundary conditions are

$$\begin{aligned} u &= 0, \quad \theta = 1, \quad \text{on } y = -1 \\ u &= 0, \quad \theta = 0, \quad \text{on } y = +1 \end{aligned} \quad (2.7)$$

3. FINITE ELEMENT ANALYSIS

To solve these differential equations with the corresponding boundary conditions, we assume if u^i, θ^i are the approximations of u , and θ we define the errors (residual) E_u^i, E_θ^i as

$$E_u^i = \frac{d}{d\eta} \left(\frac{du^i}{d\eta} \right) - (D^{-1} + M^2)u^i + \delta^2 \Delta (u^i)^2 - \delta G (\theta^i + \gamma (\theta^i)^2) \quad (2.8)$$

$$E_\theta^i = \frac{d}{dy} \left(\frac{d\theta^i}{dy} \right) - \alpha \theta^i - P N_T u^i \quad (2.9)$$

where

$$\left. \begin{aligned} u^i &= \sum_{k=1}^3 u_k \psi_k \\ \theta^i &= \sum_{k=1}^3 \theta_k \psi_k \end{aligned} \right\} \quad (3.0)$$

These errors are orthogonal to the weight function over the domain of e^i under Galerkin finite element technique we choose the approximation functions as the weight function. Multiply both sides of the equations (2.8 – 3.0) by the weight function i.e. each of the approximation function ψ_j^i and integrate over the typical three noded linear element (η_e, η_{e+1}) we obtain

$$\int_{\eta_e}^{\eta_{e+1}} E_u^i \psi_j^i dy = 0 \quad (i = 1, 2, 3, 4,) \quad (3.1)$$

$$\int_{\eta_e}^{\eta_{e+1}} E_\theta^i \psi_j^i dy = 0 \quad (i = 1, 2, 3, 4,) \quad (3.2)$$

where

$$\int_{\eta_e}^{\eta_{e+1}} \left(\frac{d}{d\eta} \left(\frac{du^i}{d\eta} \right) - D^{-1}u^i + \delta^2 \Delta (u^i)^2 - \delta G(\theta^i + \gamma \theta^{i2}) \right) \psi_j^i dy = 0 \quad (3.3)$$

$$\int_{\eta_e}^{\eta_{e+1}} \left(\frac{d}{dy} \left(\frac{d\theta^i}{dy} \right) - \alpha \theta^i - PN_T u^i \right) \psi_j^i d\eta = 0 \quad (3.4)$$

Following the Galerkin weighted residual method and integration by parts method to the equations (3.3) – (3.4) we obtain

$$\int_{\eta_e}^{\eta_{e+1}} \frac{d\psi_j^i}{dy} \frac{d\psi^i}{dy} dy - \delta D^{-1} \int_{\eta_e}^{\eta_{e+1}} u^i \psi_j^i dy + \delta^2 \Delta \int_{\eta_e}^{\eta_{e+1}} (u^i)^2 \psi_j^i dy - \delta G \int_{\eta_e}^{\eta_{e+1}} (\theta^i + \gamma \theta^{i2}) \psi_j^i dy = Q_{1,j} + Q_{2,j} \quad (3.5)$$

where – $Q_{1,j} = \Psi_j(\eta_e) \frac{du^i}{d\eta}(\eta_e)$

$$Q_{2,j} = \Psi_j(\eta_{e+1}) \frac{du^i}{d\eta}(\eta_{e+1}) \quad (3.6)$$

$$\int_{\eta_e}^{\eta_{e+1}} \frac{d\psi_j^i}{dy} \frac{d\theta^i}{dy} dy - PN_T \int_{\eta_e}^{\eta_{e+1}} u^i \psi_j^i d\eta - \alpha \int_{\eta_e}^{\eta_{e+1}} \theta^i \psi_j^i d\eta = S_{1,j} + S_{2,j} \quad (3.7)$$

where – $S_{1,j} = \Psi_j(\eta_e) \frac{d\theta^i}{dy}(\eta_e)$

$$S_{2,j} = \Psi_j(\eta_{e+1}) \frac{d\theta^i}{dy}(\eta_{e+1})$$

Making use of equations (3.0) we can write above equations as

$$\begin{aligned} \sum_{k=1}^3 u_k \int_{\eta_e}^{\eta_{e+1}} \frac{d\psi_j^i}{dy} \frac{d\psi_k}{dy} dy - \sum_{k=1}^3 \delta D^{-1} u_k \int_{\eta_e}^{\eta_{e+1}} \psi_j^i \psi_k dy - \delta G \left(\sum_{k=1}^3 \theta_k \int_{\eta_e}^{\eta_{e+1}} \psi_j^i \psi_k dy + \gamma \sum_{k=1}^3 (\theta_k)^2 (\psi_j^i)^2 \psi_k dy \right) + \\ + \delta^2 \Delta \sum_{k=1}^3 u_k^2 \int_{\eta_e}^{\eta_{e+1}} \left(\frac{d\psi_k}{d\eta} \right)^2 \psi_j^i d\eta = Q_{1,j} + Q_{2,j} \end{aligned} \quad (3.8)$$

$$\sum_{k=1}^3 \theta_k \int_{\eta_e}^{\eta_{e+1}} \frac{d\psi_j^i}{dy} \frac{d\psi_k}{dy} dy - \alpha \sum_{k=1}^3 \theta_k \int_{\eta_e}^{\eta_{e+1}} \psi_k \psi_j^i dy - PN_T \sum_{k=1}^3 u_k \int_{\eta_e}^{\eta_{e+1}} \psi_k \psi_j^i dy = S_{1,j} + S_{2,j} \quad (3.9)$$

Choosing different Ψ_j^i 's corresponding to each element η_e in the equation (3.8) yields a local stiffness matrix of order 3×3 in the form

$$(f_{i,j}^k)(u_i^k) - \delta G(g_{i,j}^k)(\theta_i^k + \gamma(\theta_i^k)^2) + \delta D^{-1}(m_{i,j}^k)(u_i^k) + \delta^2 \Delta(n_{i,j}^k)(u_i^k) = (Q_{1,j}^k) + (Q_{2,j}^k) \quad (3.10)$$

$$(l_{i,j}^k)(\theta_i^k) - P_r N_T(t_{i,j}^k)(\theta_i^k) = S_{1,j}^k + S_{2,j}^k \quad (3.11)$$

where

$(f_{i,j}^k), (g_{i,j}^k), (m_{i,j}^k), (n_{i,j}^k), (e_{i,j}^k), (t_{i,j}^k)$ are 3×3 matrices and $(Q_{2,j}^k), (Q_{1,j}^k), (R_{2,j}^k), (R_{1,j}^k), (S_{2,j}^k)$ and $(S_{1,j}^k)$ are 3×1 column matrices and such stiffness matrices (3.17) – (3.18) in terms of local nodes in each element are assembled using

inter element continuity and equilibrium conditions to obtain the coupled global matrices in terms of the global nodal values of k , θ . In case we choose n -quadratic elements then the global matrices are of order $2n+1$. The ultimate coupled global matrices are solved to determine the unknown global nodal values of the velocity, temperature and concentration in fluid region. In solving these global matrices an iteration procedure has been adopted to include the boundary and effects in the porous region.

4. STIFFNESS MATRICES

The global matrix for θ is

$$A_1 X_1 = B_1 \quad (3.12)$$

The global matrix u is

$$A_2 X_2 = B_2 \quad (3.13)$$

In fact, the non-linear term arises in the modified Brinkman linear momentum equation (3.8) of the porous medium. The iteration procedure in taking the global matrices is as follows. We split the square term into a product term and keeping one of them say u_i 's under integration, the other is expanded in terms of local nodal values as in (3.4), resulting in the corresponding coefficient matrix (n_{ij}^k) 's in (3.12), whose coefficients involve the unknown u_i 's. To evaluated (3.13) to begin with choose the initial global nodal values of u_i 's as zeros in the zeroth approximation. We evaluate u_i 's, θ_i 's in the usual procedure mentioned earlier. Later choosing these values of u_i 's as first order approximation calculate θ_i 's, In the second iteration, we substitute for u_i 's the first order approximation of and u_i 's and the first approximation of θ_i 's obtain second order approximation. This procedure is repeated till the consecutive values of u_i 's and θ_i 's differ by a reassigned percentage. For computational purpose we choose five elements in flow region.

5. DISCUSSION OF RESULTS

In this analysis we investigate the effect of quadratic density temperature variation on Non-Darcy convective heat transfer flow of a viscous fluid through a porous medium in a vertical channel in the presence of constant heat source. The equations governing the flow of heat transfer are solving by employing the Galerkin finite element analysis with quadratic approximation functions. Figures 1-5 represent the axial flow for different of G , M , D^{-1} , α and γ . Fig-1 represent variation of u with Groshof no. G it is found that the velocity is vertically down word direction and it increases with increase in G . with maximum attained at $y=-0.4$ and in this point of maximum shift towards maximum with increase in G . the variation of u with M shows that higher the Lorentz force smaller the velocity in flow region (fig -2).

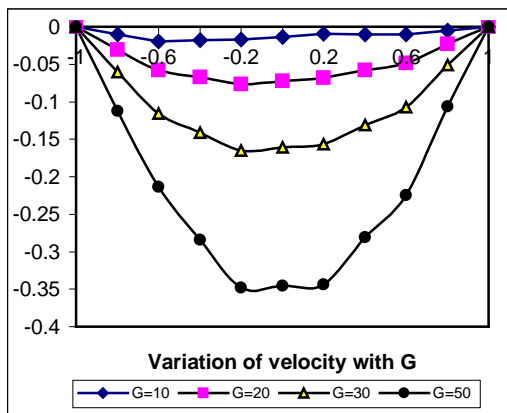


Fig. 1: Variation of u with G

	I	II	III	IV
G	10	20	30	50

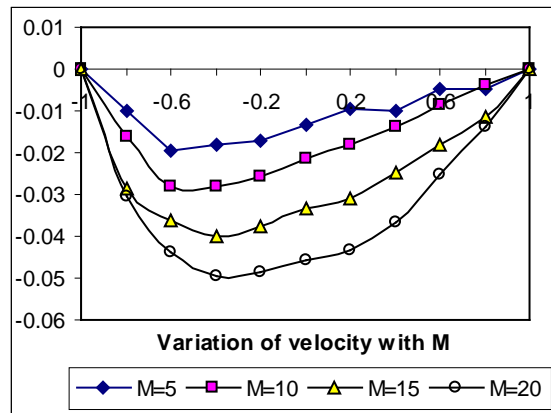


Fig. 2: Variation of u with M

	I	II	III	IV
M	5	10	15	20

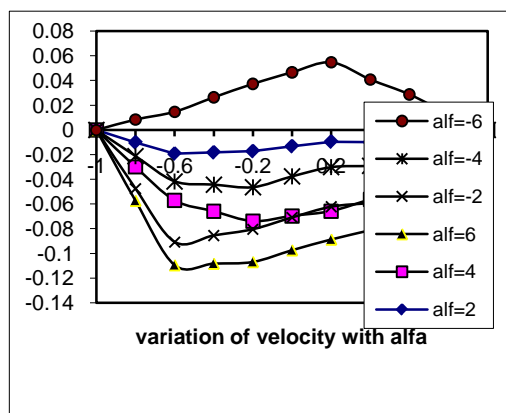


Fig. 3: Variation of u with α

	I	II	III	IV	V	VI
α	2	4	6	-2	-4	-6

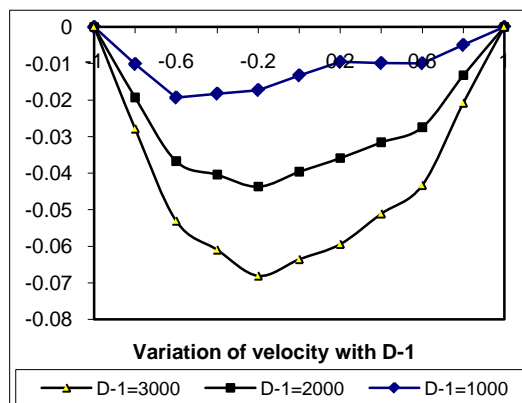


Fig. 4: Variation of u with D^{-1}

	I	II	III
D^{-1}	1×10^2	2×10^2	3×10^2

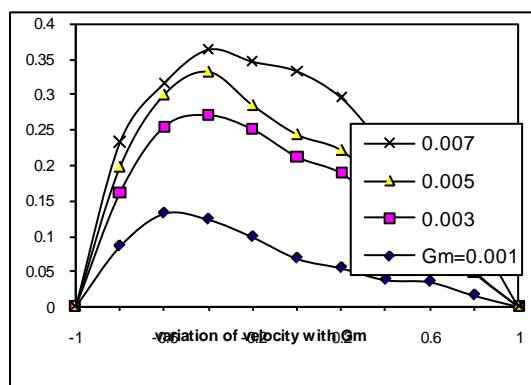


Fig. 5: Variation of u with γ

	I	II	III	I
γ	0.001	0.003	0.005	0.007

With respect to D we find that lesser the permeability of the porous medium larger the velocity in the flow region and further lower of permeability smaller $|u|$ in flow region (fig-3). The variation of u with α shows that the magnitude of u enhances with increase in the strength of heat source and enhances $|u|$ and for higher value of α . We notice a depreciation $|u|$ except in narrow region adjacent to $y=-1$ and it enhances with increase in the strength of heat sink (fig-4). The variation of density ratio γ shows that an increase in γ results depreciation in entire flow region (fig-5).

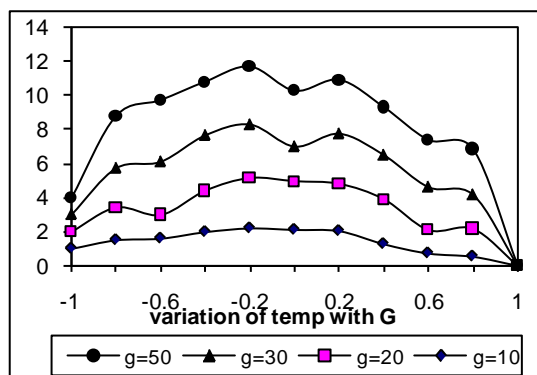


Fig. 6: Variation of θ with G

	I	II	III	IV
G	10	20	30	50

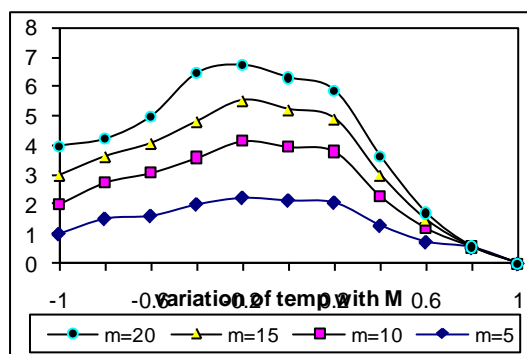


Fig. 7: Variation of θ with M

	I	II	III	IV
M	5	10	15	20

The non dimensional parameter θ is shown in figures 6-10 for different values of G , M , D^{-1} , α , γ . We follow the convention that the non dimensional temperature θ for positive or negative according as the actual temperature is greater or lesser than T_2 . fig-6 represent θ with G we found the actual temperature enhances with increase in G with maximum attained at $y=-0.2$. The variation θ with Hartmann no M shows that higher the Lorentz force lesser the actual temperature (fig-7). With respect to Darcy parameter D we found that the lesser the permeability of porous medium larger the actual temperature and further lowering of the permeability smaller the actual temperature (fig-8).

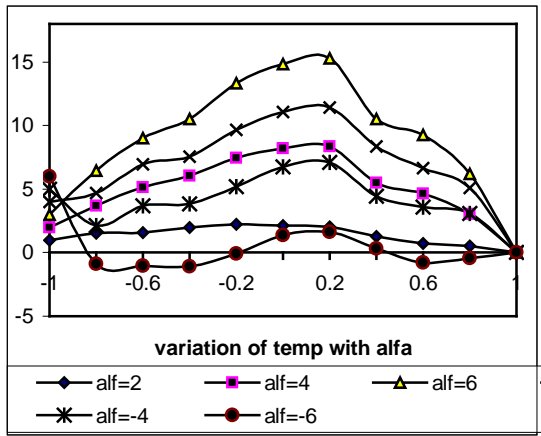


Fig. 8: Variation of θ with α

	I	II	III	IV	V	VI
α	2	4	6	-2	-4	-6

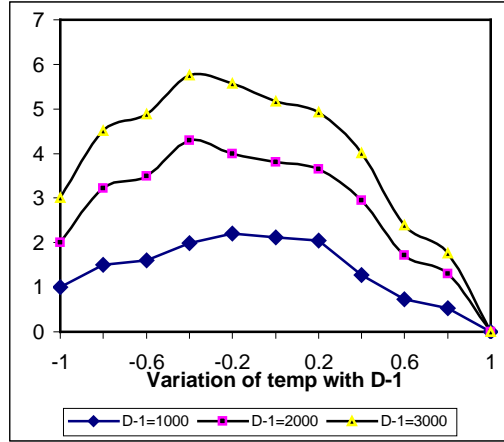


Fig. 9: Variation of θ with D^{-1}

	I	II	III
D^{-1}	1×10^2	2×10^2	3×10^2

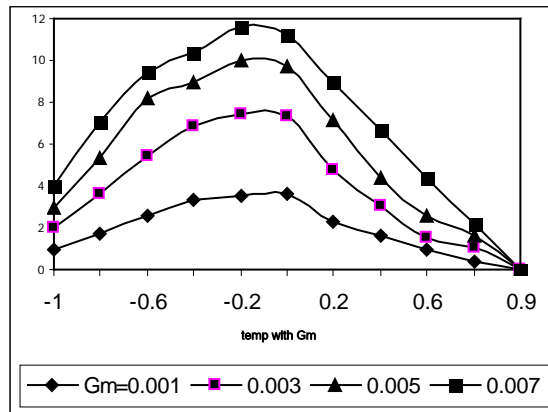


Fig. 10: Variation of θ with γ

	I	II	III	IV
γ	0.001	0.003	0.005	0.007

From fig-9 we notice that the actual temperature enhances with increase in strength of heat source and reduces with heat sink. The variation of density ratio γ is shown in fig -10 we find that the actual temperature enhances with smaller and higher values of γ and reduces with intermediate values of γ ($\gamma = 0.005$).

The shear stress at boundary layer $y = \pm 1$ is exhibited in the table 1 and 2 for different values G , D , M and γ . It is found that the τ enhances at $y = \pm 1$ with increase in G . the variation of τ with D shows that lesser the permeability of the porous medium smaller τ at $y = +1$ and at $y = -1$ smaller τ for $D \leq 2 \times 100$ and for higher $D \geq 3 \times 100$ it depreciates in magnitude. With respect to M we find that higher the Lorentz force lesser τ and for further higher the Lorentz force lesser τ at $y = 1$, while at $y = -1$ smaller τ an increase in strength of heat sources/ sink results an enhancement in τ at both walls. The variation of stress with density ratio γ shows that the stress enhances with γ at $y = +1$ and at $y = -1$ it enhances with $\gamma \leq 0.005$ and reduces with higher values at $\gamma \geq 0.007$ (table 1 and 2). The rate of heat transfer (Nusselt number) at boundary $y = \pm 1$ is exhibited in table 3 and 4 for different values. It is found that rate of heat transfer is enhanced with increase in G at both the walls. The variation of Nu with D shows that lesser the permeability of porous medium smaller the rate of heat

transfer at $y = \pm 1$. with respect to Hartmann number M we find that higher the Lorentz force smaller $Nu / (M \geq 10)$ and for further higher the Lorentz force ($M \geq 15$) larger $Nu /$ at $y=+1$ while lesser $Nu /$ at $y=-1$. An increase in strength of heat source / sink results in enhancement in the rate of heat transfer at $y = \pm 1$. The variation of Nu with density ratio γ shows that the rate of heat transfer at $y=+1$ enhances with increase in γ and at $y=-1$ it enhances with increase in $\gamma \leq 0.005$ and reduces with higher values at $\gamma \geq 0.007$.

Table-1
Shear Stress τ at $y=+1$

G	I	II	III	IV	V	VI	VII	VIII	IX	X	XI	XII	XII	IVX
10	-0.1043	-0.0998	-0.109	0.00037	0.00105	0.00038	-0.2063	-0.3122	0.1167	0.2136	0.30986	-0.1455	-0.1767	-0.20045
20	-0.2086	-0.2037	-0.193	-0.0517	0.00077	0.00191	-0.3935	-0.6123	0.2256	0.418	0.649	-0.29102	-0.38776	-0.42141
30	-0.335	-0.3014	-0.298	-0.00024	0.00302	-0.0068	-0.6386	-0.9621	0.3198	0.6312	0.9659	0.4589	-0.5250	-0.7106
50	-0.5325	-0.529	-0.533	0.00292	0.007138	0.0075	-1.1344	-1.6321	0.5669	0.0276	1.8079	-0.8527	-1.0051	-1.2199

Annexury-1

D^{-1}	1000	2000	3000	1000	1000	1000	1000	1000	1000	1000	1000	1000	1000	1000	1000
M	5	5	5	10	15	20	5	5	5	5	5	5	5	5	5
α	2	2	2	2	2	2	4	6	-2	-4	-6	2	2	2	2
γ	0.001	0.001	0.001	0.001	0.001	0.001	0.001	0.001	0.001	0.001	0.001	0.003	0.005	0.007	0.007

Table-2
Shear Stress (τ) at $y=-1$

G	I	II	III	IV	V	VI	VII	VIII	IX	X	XI	XII	XII	IVX
10	0.08195	0.0817	0.0115	0.0021	0.00087	0.00047	0.1709	0.2430	-0.1176	-0.1274	-0.2509	0.2837	0.364	0.3007
20	0.1724	0.1582	0.134	0.0099	0.00182	0.00098	0.4716	0.5994	-0.1034	-0.3462	-0.4284	0.2131	0.2723	0.1864
30	0.2044	0.2810	0.2425	0.0080	0.00263	0.00146	0.52203	0.7733	-0.2560	-0.5482	-0.5978	0.2737	0.4396	0.1595
50	0.2139	0.4152	0.2831	0.01006	0.00436	0.00249	0.7608	1.4164	-0.2615	-6.0387	-0.6799	0.3482	0.48155	0.5186

See Annexury-1

Table-3
Nusselt number (Nu1) at $y=+1$

G	I	II	III	IV	V	VI	VII	VIII	IX	X	XI	XII	XIII	IVX
10	28.2335	28.2202	28.1824	27.8763	27.8862	27.862	55.0879	81.9298	-25.623	-52.31	-79.88	28.3741	28.525	28.509
20	28.6253	28.5968	28.7367	27.5415	27.9013	27.9081	55.938	83.1738	-25.859	-53.10	-79.97	28.935	29.171	29.371
30	29.0353	28.9979	28.9429	28.0267	27.9504	27.6511	56.6873	84.3342	-26.288	-53.92	-81.40	29.524	29.841	30.061
50	29.3942	29.8003	29.6355	27.9785	28.054	28.0602	58.388	86.8562	-27.042	-55.13	-83.75	30.925	31.419	32.231

See Annexury-1

Table-2
Nusselt number Nu_2 at $y=-1$

G	I	II	III	IV	V	VI	VII	VIII	IX	X	XI	XII	XII	IVX
10	41.6821	41.6666	41.4319	41.1739	41.137	41.1158	83.2288	124.87	- 41.932	- 84.01	- 124.38	41.922	42.10	41.36
20	42.301	42.2457	43.3548	39.8246	41.17	41.1147	84.7659	126.78	- 41.847	- 84.04	- 123.88	42.43	42.97	42.03
30	42..6997	42.915	42.7596	41.4212	41.21	40.9388	85.6991	128.442	- 42.631	- 85.44	- 126.87	44.16	45.20	42.19
50	42.4765	44.001	43.4078	41.4241	41.296	41.2461	85.7374	123.228	-43.19	- 85.14	- 128.74	44.66	44.59	45.301

See Annexury-1

6. REFERENCES

1. Beckermann C.R. Viskanta and S. Ramadhyani(1986)A Numerical study of non-Darcian natural convection in a vertical enclosure filled with a porous medium, Numerical heat transfer,10,pp.557-570
2. C.L. Tien and J.T. Hong (1985). Natural convection in porous media under non-Darcian and non-uniform permeability conditions, Hemisphere, Washington D.C.
3. D.Poulikakos and A. Bejan (1985). The departure from Darcy flow in natural convection in a vertical porous layer, Physics fluids V.28, pp 3477-3484.
4. G. Lauriat and V. Prasad (1987). Natural convection in a vertical porous cavity – a numerical study for Brinkmann – extended Darcy formulation, J. Heat transfer, V.11, pp 295-320.
5. K. Vafai, R. Thyagaraju (1987). Analysis of flow and heat transfer at the interface region of a porous medium, Int J. Heat mass transfer, V.30, pp 1391-1405
6. Kalidas N and V. Prasad (1988). Benard convection in porous media effects of Darcy and Prandte numbers; Int. Symp. Convection in porous media: Non-Darcy effects, Proc. 25th Nat. Heat transfer conf., Vol.1, pp 593-604.
7. P. Cheng (1978). Heat transfer in geothermal systems, Adv. Heat transfer, 14, p 1-105.
8. P. Cheng (1987). Proc ASME/JSME Heat Transfer conf. Pp 297-303.
9. T.W. Tong and E. Subramanian (1985): A boundary layer analysis for natural convection in vertical porous enclosures – use of the Brinkman- extended darcy model, Int. J. Heat mass transfer, V.28, pp.563-571.
10. V. Prasad, F.A. Kulacki and M. keyhani (1985). Natural convection in a porous media, J. Fluid Mech. V.150, pp 89-119.
11. V. Prasad, G. Tauriat and N. Kalidas (1988): Re examination of darcy brinkman solutions for free convection in porous mediua, Int. Symp. convection in porous media: Non darcy effects, Proc. 25th Nat. Heat transfer conf. Vol. 1, pp.569-580.

Source of support: Nil, Conflict of interest: None Declared